Self-Intersection Elimination in Metamorphosis of Two-Dimensional Curves

Tatiana Samoilov and Gershon Elber
Computer Science Department
Technion
Haifa 32000, Israel
Email: {tess, gershon}@cs.technion.ac.il

June 30, 1998

Abstract

Metamorphosis, or morphing is the gradual and continuous transformation of one shape into another. The morphing problem has been investigated in the context of two-dimensional images [1], polygons and polylines [7, 9, 11], curves [2], and even voxel-based volumetric representations [8].

This work considers two methods of self-intersection elimination in metamorphosis of freeform planar curves. To begin with, both algorithms exploit the matching algorithm of [2] and construct the best correspondence of the relative parameterizations of the initial and final curves.

The first algorithm described herein, investigates building and employing a homotopy $H : [0,1] \times I\!\!R^3 \rightarrow I\!\!R^3$, where $H(t,r)$ for $t = 0$ and $t = 1$ are two given planar curves $C_1(r)$ and $C_2(r)$ and the first t parameter defines the time of fixing the intermediate metamorphosis curve. The locus of $H(t,r)$ coincides with the ruled surface between $C_1(r)$ and $C_2(r)$, but each isoparametric curve of $H(t,r)$ is self-intersection free.

The second algorithm suits morphing operations of planar curves. First, it constructs the best correspondence of the relative parameterizations of the initial and final curves. As a second post processing stage, the algorithm eliminates the remaining self-intersections and flips back the domains that self intersect.

Keywords: *Computer aided geometric design, freeform parametric curves and surfaces, homotopic curves and surfaces, matching, morphing.*

1 Introduction

The piecewise polynomial or rational curves have gained a paramount position as a representation of choice in many applications of computer graphics, geometric modeling, and vision. Probably the easiest approach to the metamorphosis of two given curves is the transformation, which is computed using a convex combination of the curves. Let $C_i(r)$, $i = 1, 2$ be two *planar simple* curves, embedded into $I\!\!R^3$,

$$C_i(r) = \{x_i(r), y_i(r), i - 1\}, \quad r \in [0,1], \quad i = 1, 2, \tag{1}$$

$$\text{where } C_i(r_1) = C_i(r_2) \quad \text{iff} \quad r_1 = r_2,$$

and let the ruled surface $R(t, r)$ be the *convex combination* of $C_1(r)$ and $C_2(r)$:

$$R(t, r) = (1 - t) \cdot C_1(r) + t \cdot C_2(r), \tag{2}$$

$$(t, r) \in \mathcal{D} = [0, 1] \times [0, 1].$$

Regrettably, this naive approach can lead to some undesirable results: varying t, the intermediate shapes during the metamorphosis process can vanish (that is, degenerate into a point) or self-intersect even if the two given curves (shapes) are self-intersection free. Hence, most of the research of metamorphosis of two-dimensional curves and three-dimensional curves and surfaces has been concentrated on the elimination of these undesired artifacts from the computed metamorphosis.

In [9] and [10], piecewise linear curves or polylines are metamorphed by deriving a *heuristic algorithm* that takes into account the angles between adjacent edges as well as the length of the edges. In [11], the geometry of both polylines is preprocessed into an intermediate representation called a *skeleton* which contains the topological information of the shape and simplifies the correspondence problem between the two shapes. In [7], *multiresolution decompositions* of the two (closed) polygons are precomputed and a metamorphosis sequence is computed between the representations in the different resolutions of two curves, only to be combined into the final metamorphosis result, in the end. In [12], one can find the attempt at the morphing of three-dimensional polyhedral models using intrinsic shape parameters.

All the above work exploits piecewise linear polygons and polylines as a representation of choice, hinting on the difficulty in extending this work to freeform curves. Even under these piecewise linear constraints, none of the above algorithms can guarantee a self-intersection free metamorphosis.

In [5], the question of the feasibility of an *automatic* metamorphosis between two freeform curves is raised. The metamorphosis, which uses a *multiresolution decomposition* (extending [7] to freeform *B-spline* curves), and the metamorphosis using *edge cutting* are considered. The latter assumes, that the highly curved regions are more likely to self-intersect during the metamorphosis stage than almost zero curvature domains, so one can attempt and reduce the curvature of the curve at the highly curved regions first.

A fundamental and related question considers the relative parameterization of the given two curves in order to avoid the undesirable effects of self-intersection or vanishing of the curves. In [2], a scheme that closely approximate the optimal relative matching between two or even n given freeform curves, under a user's prescribed norm that is based on differential properties of the curve, is represented.

In this article and following the background introduced in Section 2, two approaches of solving the self-intersection elimination problem in the metamorphosis of freeform planar curves will be presented. Both of them exploit the matching method of [2] to better form a self-intersection free morphing at the preprocessing stage. In Section 3, the first approach is presented that uses the reparameterization along the *time* domain of the ruled surface $R(t, r)$ (see Equation (2)), which is the locus of *convex combinations* of the two given curves. The second algorithm that is introduced in Section 4 suits *planar morphing operations*. Finally, we conclude in Section 5.

2 Background

Definition 1 *Let $\mathcal{S}$ be a locus of $R(t_1, r_1) = R(t_2, r_2)$, for $r_1, r_2 \in [0, 1]$ and $r_1 \neq r_2$. In other words, $\mathcal{S}$ is the locus of the self-intersection points of the ruled surface $R(t, r)$:*

$$\mathcal{S} = \{P \in R(t, r) \mid \exists r_1, r_2 \in [0, 1], \quad r_1 \neq r_2 : \; R(t_1, r_1) = R(t_2, r_2) = P\}. \tag{3}$$

In this work, we aim to guarantee that isoparametric curves $\{R(t_0, r),\ t_0 \equiv const,\ r \in [0, 1]\}$, are simple or self-intersection free.

Assumption 1 *Assume that for any point $P \in \mathcal{S}$ in the Euclidean space, there are no more than* two *different points in the parametric domain $\mathcal{D}$, which occupy P. While, in general, one can clearly find more than two points intersecting at a single point P, this case is extremely unlikely and will be ignored from now on. Furthermore, these cases of multiple coincidence may be treated in a similar way to the presented approaches.*

Hence, in the ensuing discussion, for any self-intersection point of the ruled surface $P \in R(t, r)$ there are exactly two points in the parametric domain $\mathcal{D}$, that occupy P in $I\!R^3$. Denote each such pair of points, at the same time value as *mirror points:*

Definition 2 *Two points (t, r_1) and (t, r_2) in the parametric domain $\mathcal{D}$ are* **mirror points** *iff $R(t, r_1) = R(t, r_2)$ and $r_1 \neq r_2$. Without loss of generality, assume $r_1 < r_2$. Then, (t, r_1) is called the* **left** *mirror point, and (t, r_2) the* **right** *mirror point.*

The **mirror points** have a crucial topological behavior (see Figure 1). Denote by $\bar{s_i},\ i = 1, 2, 3, 4$, the parameter values, that are small preturbations of parameters s_i. That is, $\bar{s_i} = s_i \pm \varepsilon_i$, where $\varepsilon_i,\ i = 1, 2, 3, 4$, are user's prescriptions (see Figure 1). ε_i will be employed in the coming sections for a better control over the elimination of the self-intersections. Then,

Definition 3 *Consider the isoparametric curve $C(s) = R(t_0, s)$ of the ruled surface $R(t, s)$, where $s \in [0, 1], t_0 \equiv const$, and s is an* arc length *parameterization.*

If $\{(t_0, s_1), (t_0, s_2)\}$ and $\{(t_0, s_3), (t_0, s_4)\}$, $s_1 < s_3 < s_4 < s_2$ are two adjacent pairs of two

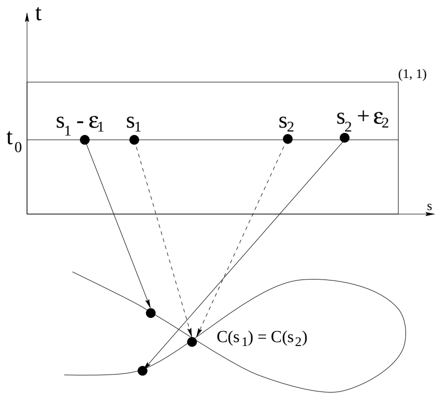

Figure 1: Mirror points (t_0, s_1) and (t_0, s_2). $\bar{s_1} = s_1 - \varepsilon_1$, $\bar{s_2} = s_2 + \varepsilon_2$.

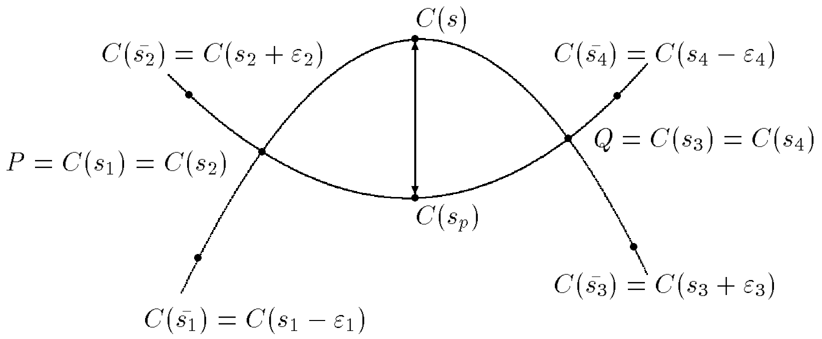
$C(s)$
$C(\bar{s_2}) = C(s_2 + \varepsilon_2)$
$C(\bar{s_4}) = C(s_4 - \varepsilon_4)$
$P = C(s_1) = C(s_2)$
$Q = C(s_3) = C(s_4)$
$C(s_p)$
$C(\bar{s_3}) = C(s_3 + \varepsilon_3)$
$C(\bar{s_1}) = C(s_1 - \varepsilon_1)$

Figure 2: Shown are two *parallel segments* of the curve $C(s)$, $[C(\bar{s_1}), C(\bar{s_3})]$ and $[C(\bar{s_2}), C(\bar{s_4})]$, where $s_1 < s_3 < s_4 < s_2$, $P = C(s_1) = C(s_2)$ and $Q = C(s_3) = C(s_4)$ are the two **mirror points**, and $C(s)$ and $C(s_p)$ are the two *parallel points.*

mirror points *on* $C(s)$, $P = C(s_1) = C(s_2)$ *and* $Q = C(s_3) = C(s_4)$, *then the segments* $[C(\bar{s_1}), C(\bar{s_3})]$ *and* $[C(\bar{s_4}), C(\bar{s_2})]$ *of the curve* $C(s)$ *are denoted as* **parallel segments** *(see Figure 2).*

Definition 4 *If* $[C(\bar{s_1}), C(\bar{s_3})]$ *and* $[C(\bar{s_4}), C(\bar{s_2})]$ *are the* parallel segments *of the curve* $C(s)$, *then for any* $s \in [\bar{s_1}, \bar{s_3}] \cup [\bar{s_4}, \bar{s_2}]$ *the* **parallel point** *of* s, s_p *(see Figure 2) is defined as:*

$$s_p = \begin{cases} \bar{s_2} - \frac{(s-\bar{s_1})\cdot(\bar{s_2}-\bar{s_4})}{\bar{s_3}-\bar{s_1}} & \textit{if } \bar{s_1} \le s \le \bar{s_3}, \\ \bar{s_1} + \frac{(\bar{s_2}-s)\cdot(\bar{s_3}-\bar{s_1})}{\bar{s_2}-\bar{s_4}} & \textit{if } \bar{s_4} \le s \le \bar{s_2}. \end{cases} \tag{4}$$

Section 2.1 considers a method to locate the set $\mathcal{S}$, or the self-intersection points of the ruled surface $R(t, s)$ between two planar curves $C_1(r)$ and $C_2(r)$ (see Figure 3).

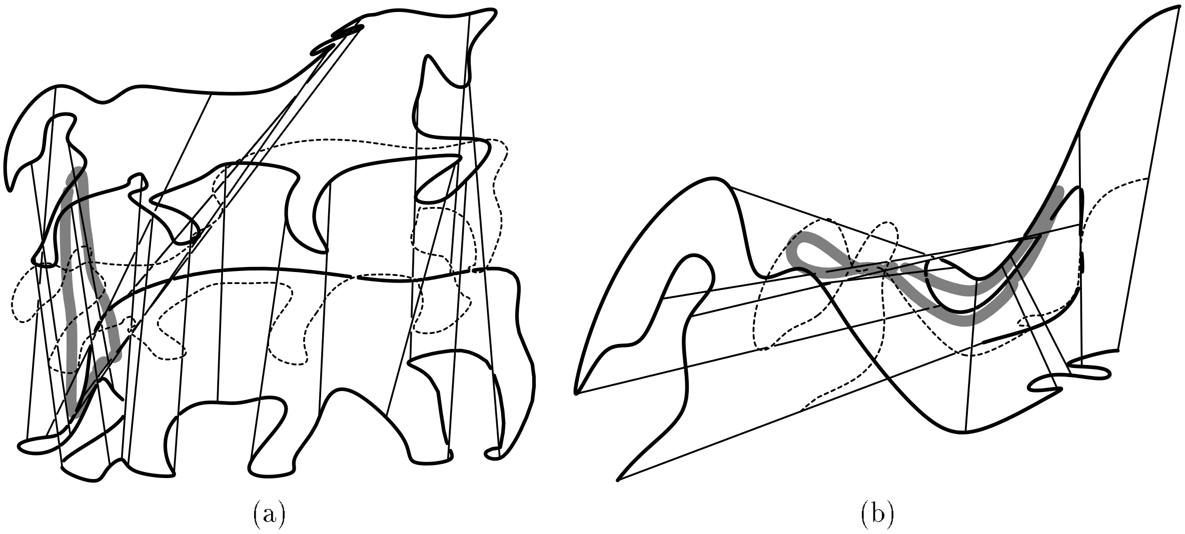

Figure 3: Self-intersection on the ruled surface between a horse (top in (a)) and an elephant (bottom in (a)). The resulting ruled surface between the two outlines self intersects. The resulting self intersection curve, near the tail, is shown in (a) in gray color. Also shown in (a), in a dotted line style, is one intermediate isoparametric curve of this ruled surface that self intersects near the tails. (b) shows an enlarged view of the self-intersection area between the two tails.

2.1 Self-Intersection Curves of $R(t,s)$

We are interested in the elimination of the *self-intersections* in the ruled surface $R(t,r)$ between $C_1(r)$ and $C_2(r)$, when they occur for the *same* value of the parameter t, and different values of the parameter r.

Lemma 1 *$R(t,r_1) = R(t,r_2)$, $(t,r_1),(t,r_2) \in \mathcal{D}$, iff there exist $d < 0$ such that,*

$$(C_1(r_1) \; - \; C_1(r_2)) = d \cdot (C_2(r_1) \; - \; C_2(r_2)). \tag{5}$$

Proof: For $t = 0$ or $t = 1$, $R(t,r)$ does not self-intersect, since $C_1(r)$ and $C_2(r)$ are known to be simple curves.

If $R(t,r_1) = R(t,r_2)$ for some $t \in (0,1)$, then

$(1-t)\cdot C_1(r_1) + t \cdot C_2(r_1) = (1-t)\cdot C_1(r_2) + t \cdot C_2(r_2)$,

or, in other words,

$C_1(r_1) - C_1(r_2) = \frac{t}{1-t} \cdot (C_2(r_1) - C_2(r_2))$.

Let d be $\frac{t}{t-1}$. Then, for $t \in (0,1)$ we have $d < 0$, $t = \frac{d}{d-1}$ and $(C_1(r_1) - C_1(r_2)) = d \cdot (C_2(r_1) - C_2(r_2))$.
■

Recall that the curves $C_1(r)$ and $C_2(r)$ are planar. Then, we have: $R(t_1,r_1) = R(t_2,r_2)$ iff $t_1 = t_2 = \frac{d}{d-1} \in (0,1)$ and Equation (5) holds.

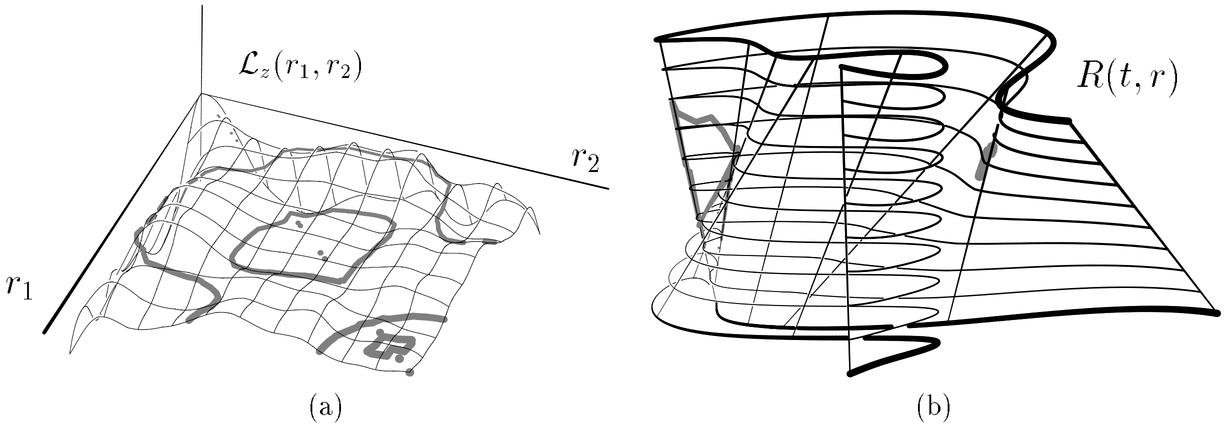

Figure 4: In (a), the z component of the symbolically computed vector field of $\mathcal{L}(r_1, r_2)$ is shown. The zero set of $\mathcal{L}_z(r_1, r_2)$ is also shown in (a) in a gray color. This zero set is employed in (b) to detect the self-intersections (in gray color) in the original surface $R(t, r)$.

Corollary 1 *The condition of Lemma 1 is equivalent to:*

$$R(t, r_1) = R(t, r_2), \quad \forall (t, r_1), (t, r_2) \in \mathcal{D},$$

iff,

$$\mathcal{L}(r_1, r_2) = (C_1(r_1) - C_1(r_2)) \times (C_2(r_1) - C_2(r_2)) = \begin{pmatrix} 0 \\ 0 \\ 0 \end{pmatrix} \tag{6}$$

and,

$$\langle C_1(r_1) - C_1(r_2), C_2(r_1) - C_2(r_2) \rangle \leq 0.$$

Assume, $C_i(r)$ are constant z curves. Then, the surface $\mathcal{L}(r_1, r_2)$ has only one *non zero* component, *i.e.* $\mathcal{L}_x(r_1, r_2) \equiv \mathcal{L}_y(r_1, r_2) \equiv 0$, $\forall r_1, r_2 \in [0, 1]$.

In order to detect and compute *all* self-intersection points of the ruled surface $R(t, r)$, $\mathcal{L}(r_1, r_2)$ is symbolically computed from the bivariate vector fields of the two surfaces of $S_1(r_1, r_2) = C_1(r_1) - C_1(r_2)$ and $S_2(r_1, r_2) = C_2(r_1) - C_2(r_2)$ (see [6]), and the *zero set* of the z component of the surface $\mathcal{L}(r_1, r_2) = S_1(r_1, r_2) \times S_2(r_1, r_2)$, $\mathcal{L}_z(r_1, r_2)$ is derived resulting in the set $\mathcal{S}$ (see Figure 4).

Once the zero set of $\mathcal{L}_z(r_1, r_2)$ has been computed, One can derive d using Equation (5) and then derive t. With the computed t, the self-intersection points in $\mathbb{R}^3$ can clearly be derived as $(1-t)C_1(r_i) + tC_2(r_i)$, $i = 1, 2$. Figure 4 (a) shows $\mathcal{L}_z(r_1, r_2)$ as well its zero set along with the self intersection in $\mathbb{R}^3$ in Figure 4 (b).

The matching algorithm for freeform curves of [2] between the two given curves, is applied in both algorithms that are described in the following Section 3 and Section 4 as a preprocessing stage. It is com-

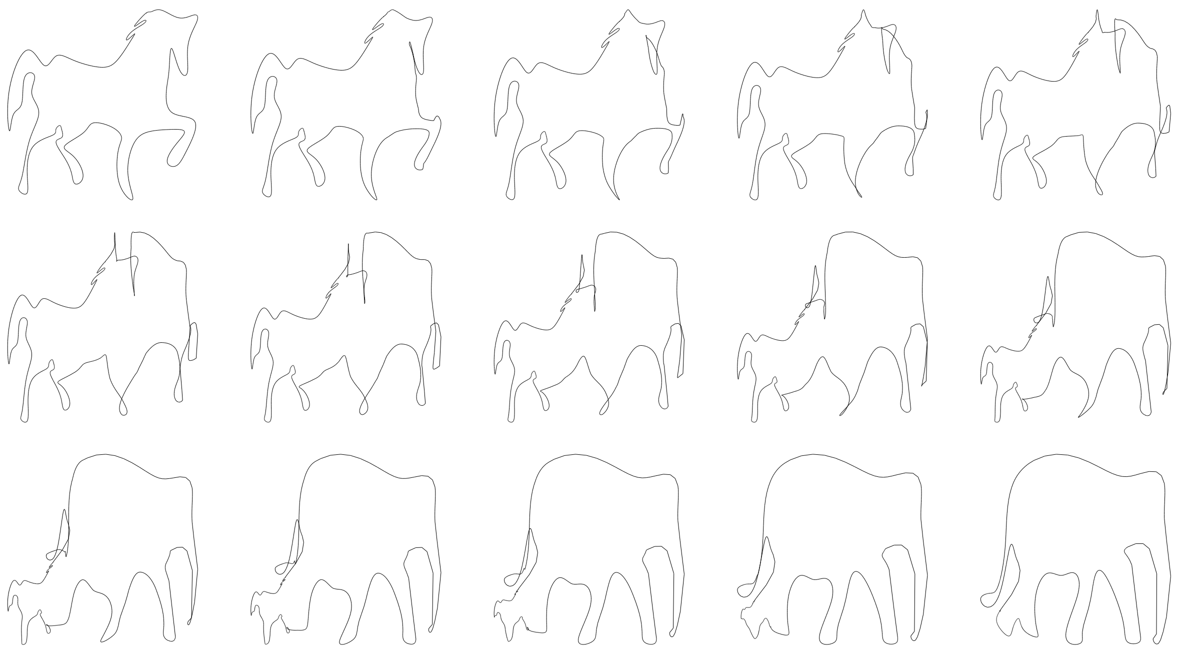

Figure 5: A Morphing sequence between an elephant (bottom right) and a horse (top left), using a naive convex combination of the initial and final curves $(1-t) \cdot C_1(r) + t \cdot C_2(r)$. Compare with Figure 6.

pletely automatic and has been successfully employed in different metamorphosis applications of freeform curves with feature preservations. The usefulness of the approach of [2] can be appreciated by comparing Figures 5 and 6. Section 2.2 describes the basic scheme of [2].

Creating *intermediate* curves as *convex combinations* of the two input curves, $C(r) = R(t_0, r), t_0 \in [1, 0]$, following Equation (2), one should correct for remaining self-intersections, if such occur. The self-intersection elimination stage is discussed in Sections 3 and 4. The algorithms described in these section use the freeform curve matching algorithm of [2] that is briefly reviewed in Section 2.2.

2.2 Matching of Freeform Curves

The algorithm of [2] matches the relative parameterizations of two or more freeform parametric curves, using their first order differential properties. In our case, it is enough to use only the *tangent fields* of the given curves, the unit vectors $T_1(r) = \frac{C_1'(r)}{||C_1'(r)||}$ and $T_2(v) = \frac{C_2'(r)}{||C_2'(r)||}$.

Consider the inner product of the unit tangent vectors. When the inner product of $T_1(r)$ and $T_2(r)$ is maximal, that is $\langle T_1(r), T_2(r)\rangle = 1$, then the tangent vectors of $C_1(r)$ and $C_2(r)$ are parallel at r. If the *tangents* of the curves are parallel throughout the entire parametric domain, then $\langle T_1(r), T_2(r)\rangle = 1, \forall r \in [0, 1]$, and we say that the two curves are *completely matched.* Typically, this is not the case and one only requires the inner product of the tangent vectors to be positive throughout the curve's parameterization, $\langle T_1(r), T_2(r)\rangle > 0, \ \forall r \in [0, 1]$, creating a *valid* parameterization. By Lemma 1, it is clear, that no self-

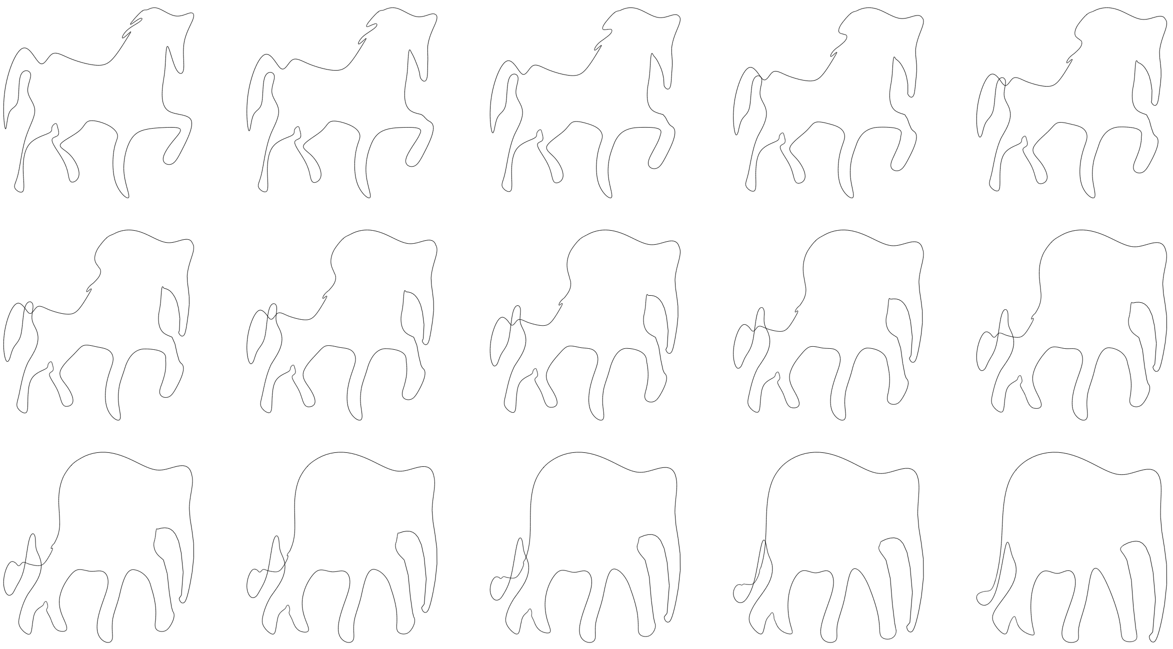

Figure 6: A Morphing sequence between an elephant (bottom right) and a horse (top left), using convex combination of the initial and final curves after the application of the *curve matching algorithm* [2]. Compare with Figure 5. Note the remaining self-intersection near the tail.

intersection can occur in the intermediate metamorphed curves if the parameterization of the initial curves is *valid.* Therefore, one can reformulate the reparameterization problem, by maximizing the following functional:

$$\max_{v(u)} \int_0^1 \langle T_1(u), T_2(v(u)) \rangle \, du, \quad v(0) = 0, \ v(1) = 1,$$

where $v(u)$ is a regular change of parameter.

If a *valid match* between the two given curves exists, then the algorithm of [2] guarantees not only to find a match, but also to compute the best match out of the set of possible *valid matching.* Figure 6 is the result of exploiting this algorithm. Compare it with the Figure 5.

Regrettably, the algorithm cannot prevent self-intersections if no valid match can be established. Moreover, this algorithm cannot eliminate global self-intersections as in Figure 6. In such cases, one must correct the results, using some other approaches, two of which are described in this paper in the coming sections.

3 The Time Variance Algorithm

All of metamorphosis methods that were discussed in Section 1 employ continuous transformations, that can be considered as homotopic transformations $\bar{H} : [0, 1] \times I\!R^3 \longrightarrow I\!R^3$, where the first parameter coincides with the *time* of fixing the curve. For metamorphing of curves, we have: $H : [0, 1] \times [0, 1] \longrightarrow I\!R^3$, where

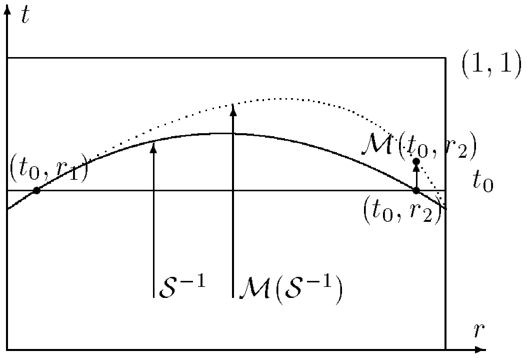

Figure 7: Suppose that $\mathcal{S}^{-1} = \{(t,r) \in \mathcal{D} \mid R(t,r) \in \mathcal{S}\}$, (t_0, r_1) and (t_0, r_2) are two mirror points in the *parametric domain* $\mathcal{D}$, such that $R(t_0, r_1) = R(t_0, r_2) = R \circ \mathcal{M}(t_0, r_1) \neq R \circ \mathcal{M}(t_0, r_2)$.

the second parameter corresponds to the parameter on the given curves.

Herein, the homotopy $H(t, r)$ connects the two given curves in the three-dimensional space and lies on the *ruled surface* $R(t, r)$ between the given curves – that is $H(t,r) = R \circ \mathcal{M}(t,r)$, were $\mathcal{M}(t,r)$ is some surjective continuous function $\mathcal{M} : \mathcal{D} \longrightarrow \mathcal{D}$, satisfying the following condition: if (t_0, r_1), $(t_0, r_2) \in \mathcal{D}$ are two mirror points of $R(t,r)$, then $R \circ \mathcal{M}(t_0, r_1) \neq R \circ \mathcal{M}(t_0, r_2)$. The graph of the convex combination of the given curves is identical to the graph of the surface $R \circ \mathcal{M}(t,r)$. Nevertheless, for any given $t \in [0,1]$, the Euclidean location of the point $R \circ \mathcal{M}(t,r)$ may be different from $R(t,r)$ in order to avoid the cases of self-intersections of the curve $H(t_0, r)$, at any given $t_0 \in [0,1]$.

We seek a C^0 continuous surjective deformation $\mathcal{M} : \mathcal{D} \longrightarrow \mathcal{D}$, that satisfies the following conditions (see Figure 7):

1. If $(t_0, r_1), (t_0, r_2) \in \mathcal{D}$ are two mirror points of $R(t,r)$, then $R \circ \mathcal{M}(t_0, r_1) \neq R \circ \mathcal{M}(t_0, r_2)$.
2. $\mathcal{M}(t,r) = (t,r), \forall r \in [0,1]$, $t = 0, 1$, two initial boundary conditions on $C_i(r)$, $i = 1, 2$.
3. If $C_i(r)$, $i = 1, 2$ are closed curves, then $\mathcal{M}(t, 1) = \mathcal{M}(t, 0)$, $\forall t \in [0,1]$. Continuity condition for periodic closed curves.

One possible simple construction for this $\mathcal{M}$ deformation follows. Let (t_0, r_1), $(t_0, r_2) \in \mathcal{D}$ be *mirror points*, $r_1 < r_2$ and let $r_{12} = \frac{r_1 + r_2}{2}$. Then:

$$\mathcal{M}(t_0, r) = \begin{cases} (t_0, r) & \text{if } r \leq r_{12}, \\ (\lambda(t_0, r), r) & \text{otherwise}, \end{cases} \tag{7}$$

where $\lambda : \mathcal{D} \longrightarrow [0,1]$ (see Figure 8) is selected to be a C^0 continuous increasing function of the first *time*

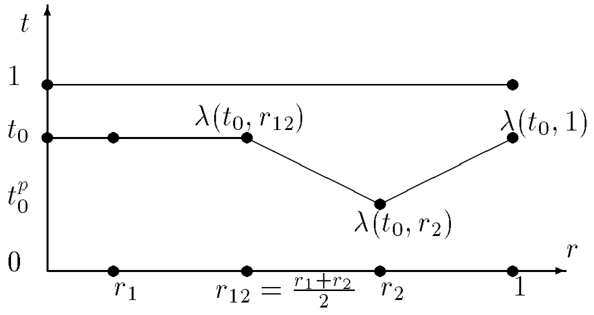

Figure 8: $\lambda(t_0, r),\ t_0 \equiv const,\ r \in [0, 1]$.

parameter, for any fixed value of the second parameter r and any $p > 0$:

$$\lambda(t,r) = \begin{cases} t, & \text{if } r \le r_{12}, \\ \frac{r_2 - r}{r_2 - r_{12}} \cdot t + \frac{r - r_{12}}{r_2 - r_{12}} \cdot t^p, & \text{if } r_{12} \le r \le r_2, \\ \frac{r - r_2}{1 - r_2} \cdot t + \frac{1 - r}{1 - r_2} \cdot t^p, & \text{if } r_2 \le r \le 1. \end{cases} \tag{8}$$

Function $\lambda(t, r)$ may be non linear or even a *Bézier* or a *B-spline* function of r. $\lambda(t, r)$ is an allowable change of the parameter for any $r \equiv const$ isoparametric curve of the ruled surface $R(t, r)$.

Inspecting $R \circ \mathcal{M}(t, r)$, the geometric shape of $R(t, r)$ is completely preserved by the deformation, so $\mathcal{S}$ continues to be the locus of self-intersection points of $R \circ \mathcal{M}(t, r)$.

Nevertheless, following the deformation $\mathcal{M}$, all existing *mirror points* in $R(t, r)$ would vanish, effectively removing these self-intersections from the isoparametric curves of $R(t_0, r), t_0 \equiv const$. Yet, one should recall that these isoparametric curves are only intermediate steps in the planar curves' metamorphosis, and are now *three-dimensional*. One need to project these three-dimensional curves onto the XY plane.

Figure 10 shows a naive metamorphosis sequence, generated using convex combination of the tail of the elephant and the horse (with parameterization that differes slightly from the one of whole animals) from Figure 6. Figure 11 shows the projection of these curves on XY plane after the application of the reparameterization function $\mathcal{M}(t, r)$.

Hence, expecting the intermediate curves of the morphing process to be *planar* as well, one must find some projections to the plane, that preserve the self-intersection free property in the intermediate *three-dimensional* curves and provide the entire metamorphosis sequence in the two-dimensional plane. Section 3.1 considers several such projections.

3.1 Projections

One simple projection to a plane, could be an orthogonal projection of the three-dimensional non planar curve onto some plane $\mathcal{P}$ along a projection direction that would guarantee a self-intersection free curve (see Figure 9), in each of the intermediate curves. Then, it might be possible to find a continuous transition

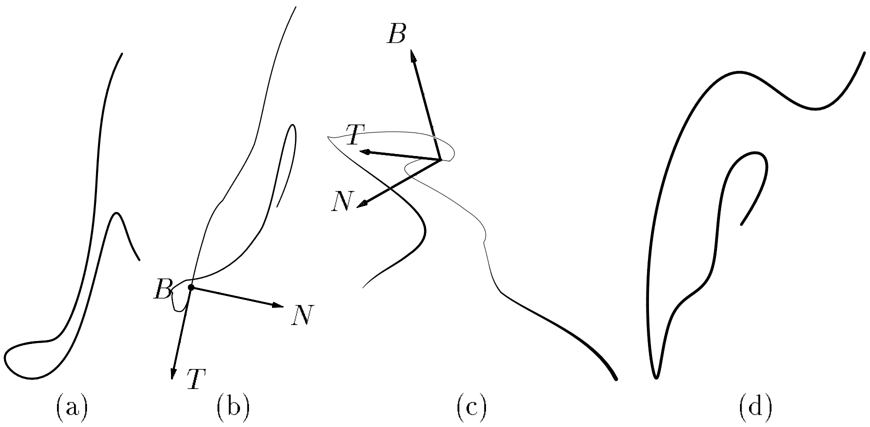

Figure 9: (a) and (d) are the tails on the initial and final curves of $R(t, r)$ from Figure 3 of the elephant and the horse respectively, (b) shows one of the isoparametric curves of $R \circ \mathcal{M}(t_0, r)$, $t_0 \equiv const$, $r \in [0, 1]$, after the deformation $\mathcal{M}$ has been applied to $R(t, r)$, and (c) is the orthogonal planar projection of the curve (b), that is self-intersection free. The *Frenet frame* shown in (b) and (c) can be used as well as a non linear projection along the binormal direction $B(s)$.

of such planes as a function of the *time*, t. The homotopy would consist of the composition of $R \circ \mathcal{M}(t, s)$ and projections onto a set of continuous planes $\mathcal{P}(t)$.

Unfortunately, this method is difficult to use. Such planes are not guaranteed to exist for a whole composed curve, $R \circ \mathcal{M}(t_0, r)$, enabling a projection that is self-intersecting free. Other Possible alternatives may be,

1. Consider the projection of the curve $C(r)$, $C : [0, 1] \longrightarrow I\!R^3$, onto its osculating plane, which moves along the curve together with the *modified Frenet Frame*, which rotates smoothly at inflection points [3]. See Figure 9.

2. Assign for each point of the curve $C(r)$ a vector $V(r)$, to be used as the *projection direction.* $V(r)$ must be orthogonal to the *tangent plane* of the segments, where the curve is *planar*, in order to preserve the geometric features of these parts of the curve. These *projection directions* can be set as a vector field, $V(r)$, for $C(r) = R(t_0, r)$, the curve could be projected to some plane along the corresponding vectors in $V(r)$. Interestingly enough, the placement of the plane of the planar projection has a significant effect on the end result, including the delineation between the ability to eliminate self-intersections and their possible existence. If the *projection direction* is equal to the *binormal* vector field, $B(r)$ (see [4]), of the curve $C(r)$ (see Figure 9), methods 1 and 2 coincide.

3. Define the *projection direction* $V(s)$ as $V(s) = T(s) \times [C(s_p) - C(s)]$, where $T(s)$ is the *tangent vector of* $C(s)$ and points s and s_p are *parallel* (see Definition 4).

In Figures 10, 11 and 12, one can find an example of the metamorphosis of the two tails from Figure 6

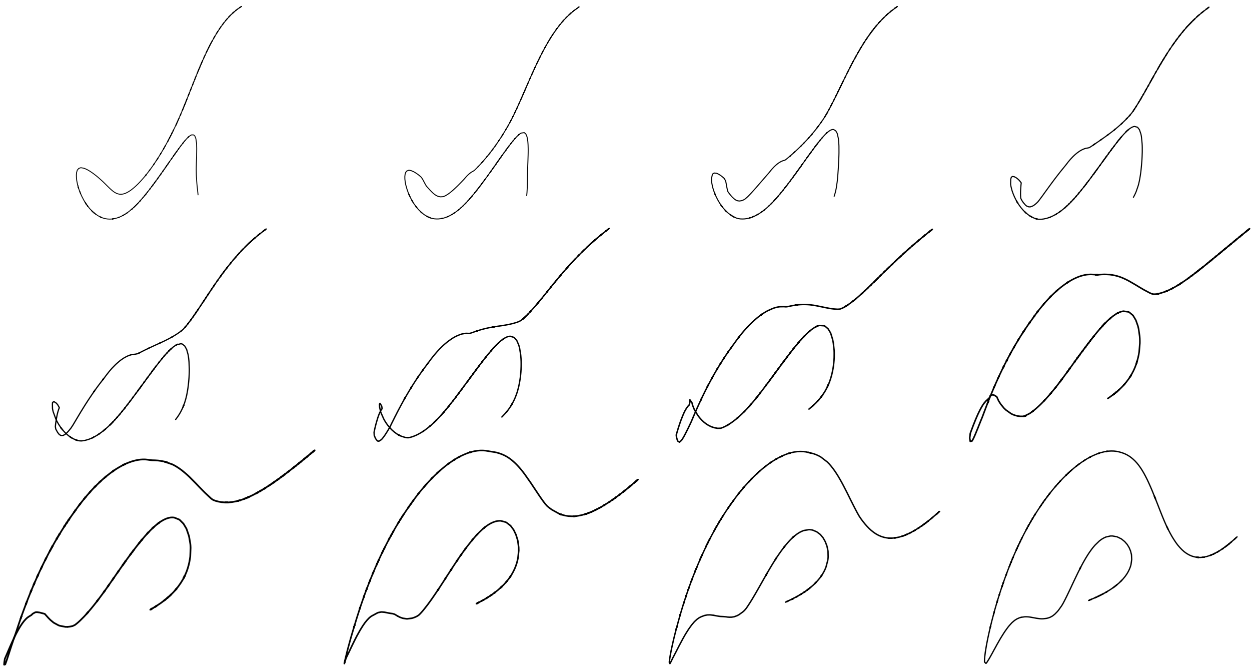

Figure 10: A Morphing sequence between the tails of the elephant (top left) and the horse (bottom right) using a naive convex combination of the initial and final curves $(1-t)\cdot C_1(r)+t\cdot C_2(r)$. Compare with Figures 11 and 12.

that were generated with the aid of the time variance algorithm after an orthogonal projection along a set of planes $\mathcal{P}(t)$, when the $\mathcal{P}(t)$ is defined by the following:

$$\mathcal{P}(t)=\begin{cases}\mathcal{P}_0, & \text{if } 0\le t\le t_1\\ \mathcal{P}_0\cdot\frac{t_{12}-t}{t_{12}-t_1}+\mathcal{P}_1\cdot\frac{t-t_1}{t_{12}-t_1}, & \text{if } t_1\le t\le t_{12}\\ \mathcal{P}_1\cdot\frac{t_2-t}{t_2-t_{12}}+\mathcal{P}_2\cdot\frac{t-t_{12}}{t_2-t_{12}}, & \text{if } t_{12}\le t\le t_2\\ \mathcal{P}_0\cdot\frac{t-t_2}{1.0-t_2}+\mathcal{P}_2\cdot\frac{1.0-t}{1.0-t_2}, & \text{if } t_2\le t\le 1\end{cases}\tag{9}$$

where

$$\mathcal{P}_0=\{(x,y,z)\in I\!R^3|\ z=0\},$$

$$\mathcal{P}_1=\{(x,y,z)\in I\!R^3|\ 0.439\cdot x-0.415\cdot y+0.797\cdot z=0\},$$

$$\mathcal{P}_2=\{(x,y,z)\in I\!R^3|\ 0.356\cdot x-0.545\cdot y+0.759\cdot z=0\},$$

and $t_1=\frac{1}{3}$, $t_2=\frac{5}{8}$, $t_{12}=\frac{t_1+t_2}{2}$.

4 The Flipping Algorithm

The second approach at self-intersection elimination assumes the metamorphosis of *planar* curves. One can start by applying the matching algorithm for freeform curves of [2] between the two given curves (see

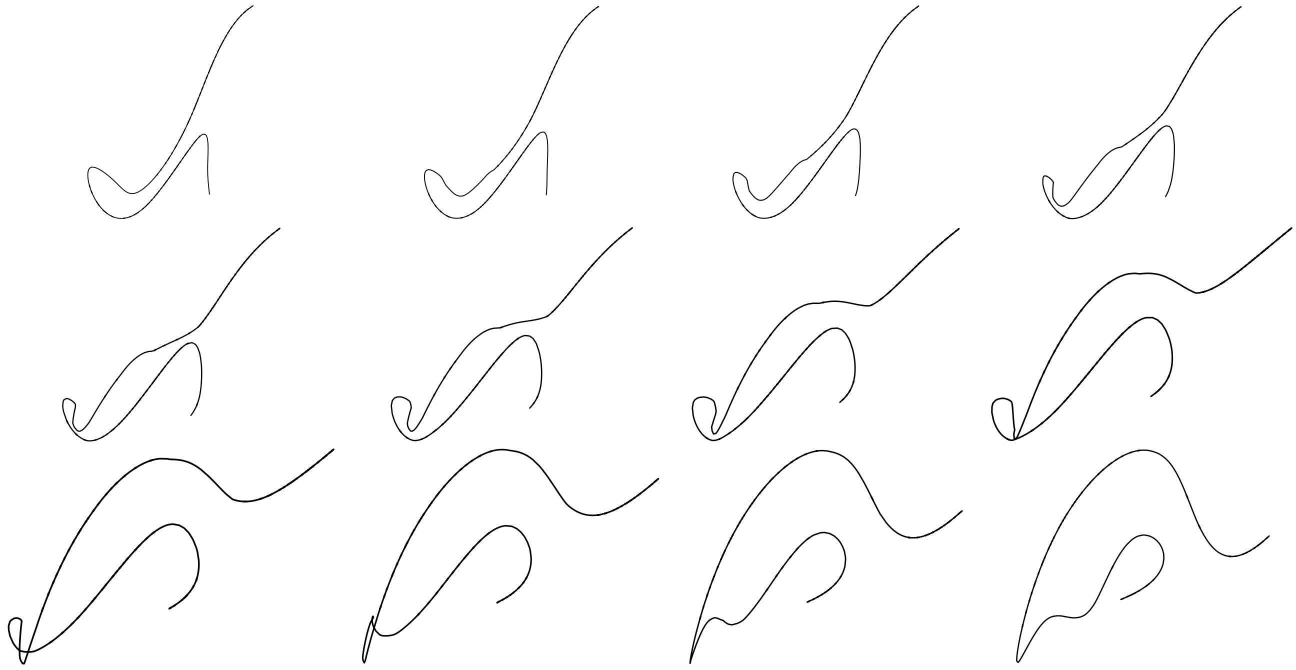

Figure 11: A Morphing sequence between the tails of the elephant (top left) and the horse (bottom right) using a naive convex combination of the initial and final curves $(1-t)\cdot C_1(r)+t\cdot C_2(r)$ after the time variance algorithm. Compare with Figures 10 and 12. Note, this figure is an orthogonal projection of 3D curves.

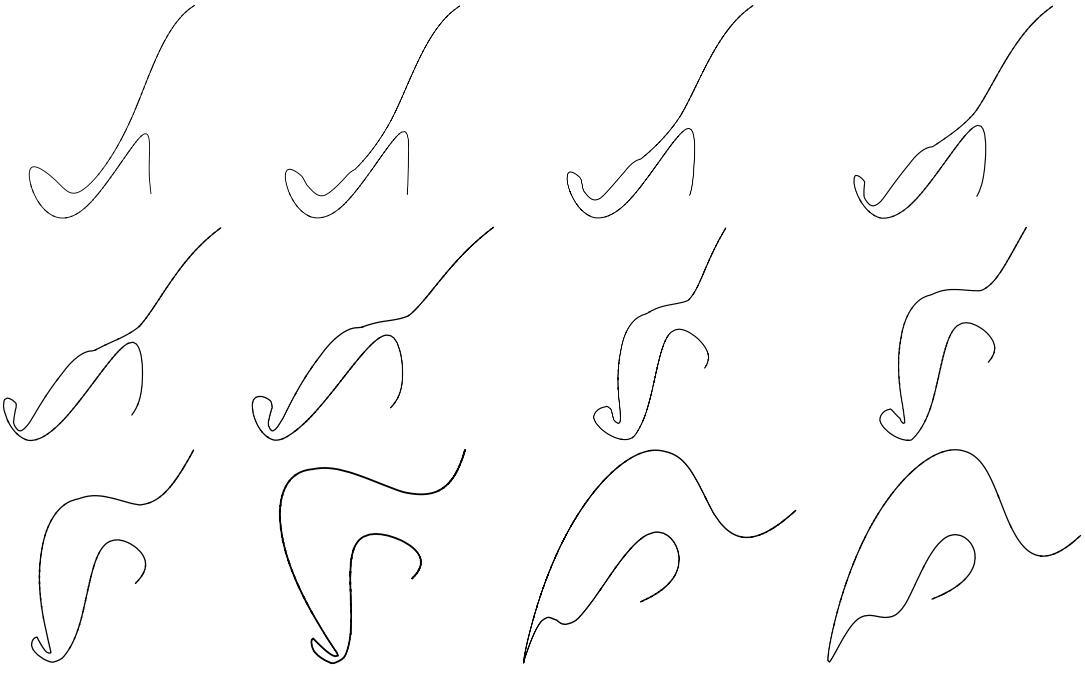

Figure 12: A Morphing sequence between the tails of the elephant (top left) and the horse (bottom right) using a naive convex combination of the initial and final curves $(1-t)\cdot C_1(r)+t\cdot C_2(r)$ after the time variance algorithm and the orthogonal projection on the set of continuous planes $\mathcal{P}(t)$, described in the Equation (9). Compare with Figures 10 and 11.

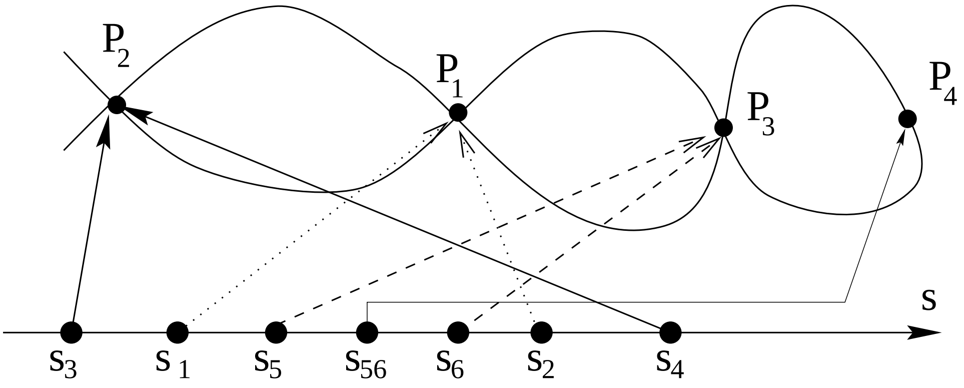

Figure 13: In this figure three points of $\mathcal{S}$ can be found on the isoparametric curve $C(s) = R(t_0, s)$, $t_0 \equiv const$, $s \in [0, 1]$: $P_1 = C(s_1) = C(s_2)$, $P_2 = C(s_3) = C(s_4)$ and $P_3 = C(s_5) = C(s_6)$, where $s_3 < s_1 < s_5 < s_6 < s_2 < s_4$, the fourth point $P_4 = C(\frac{s_5+s_6}{2})$ is selected to form the second pair of self-intersection points.

Section 2.2). Regrettably, as we have seen before, this algorithm cannot guarantee self-intersection free metamorphosis of the two given planar curves. A second self-intersection elimination method is presented in this Section.

4.1 Self-Intersections Elimination

We are interested in modifying only the curves, that contain self-intersections, and only in a local way, preserving the well behaved regions of the curve. The following method is automatic, and can be effectively used with any regular planar curve. It provides the user with the freedom to set the domain of the curve, which will be affected by the algorithm, and the minimal distance between the end points of the **parallel segments**, of the curve, affected by a correction amount and arc length of the deformation: $\xi = \min\{||R(t_0, \bar{s_1}) - R(t_0, \bar{s_2})||, ||R(t_0, \bar{s_3}) - R(t_0, \bar{s_4})||\}$ and $\zeta = \max_i\{\varepsilon_i\}$ (see Figure 2). The end result is controlled via the modifications of these degrees of freedom (compare Figure 16 and Figure 17).

The flipping algorithm operates in two phases. First, the algorithm finds pairs of two-dimensional points in $\mathcal{S}$, and orders them according to the value of the arc length parameter s of the curve. If P_1, P_2, $P_3 \in \mathcal{S}$ and $P_1 = R(t_0, s_1) = R(t_0, s_2)$, $P_2 = R(t_0, s_3) = R(t_0, s_4)$, and $P_3 = R(t_0, s_5) = R(t_0, s_6)$, where $s_3 < s_1 < s_5 < s_6 < s_2 < s_4$, then the first selected pair is $\{P_2, P_1\}$ (see Figure 13 (a)). If there is only odd number of such mirror points, $P_4 = R(t_0, s_7) = R(t_0, s_8) \in \mathcal{S}$, then the second point, which will be selected for the last pair, will be $P_5 = R(t_0, \frac{s_7+s_8}{2})$ (see Figure 13 (b)).

In the second phase, one selects a smooth functions $\mathcal{F}$ to flip the **parallel segments** of the curve, corresponding to these pairs of mirror points.

For example, if the selected pair is $\{P_2, P_1\}$, where $P_1 = R(t_0, s_1) = R(t_0, s_2)$, $P_2 = R(t_0, s_3) =$

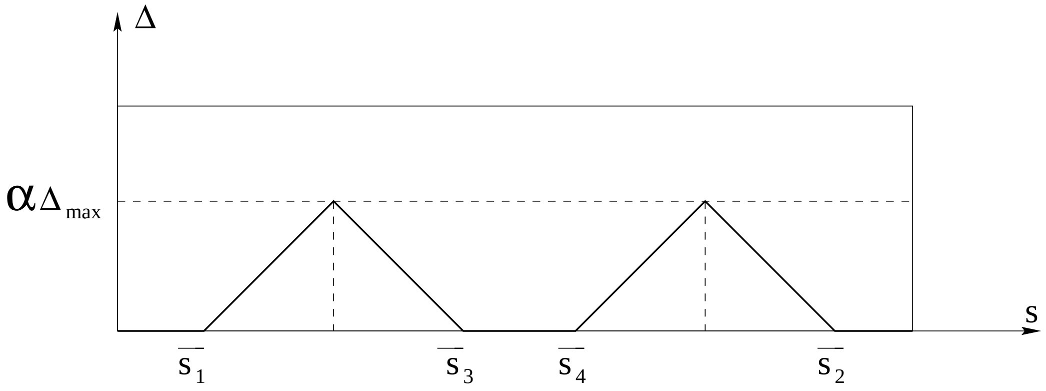

Figure 14: $\Delta(s)$ function for the **parallel segments** $[\bar{s_1}, \bar{s_3}]$ and $[\bar{s_4}, \bar{s_2}]$.

$R(t_0, s_4), s_3 < s_1 < s_2 < s_4$, then $\mathcal{F}$ may be defined in the following way:

$$\mathcal{F} \circ R(t_0, s) = R(t_0, s) + \Delta(s) \cdot (R(t_0, s) - R(t_0, s_p)),$$

where s_p is a *parallel point* of s. Let $\Delta_{max} = ||R(t_0, \frac{s_1+s_3}{2}) - R(t_0, \frac{s_2+s_4}{2})||$. Then,

$$\Delta(s) = \begin{cases} \alpha \cdot \left[1 - |\frac{2 \cdot s - (\bar{s_1} + \bar{s_3})}{\bar{s_1} - \bar{s_3}}|\right] \cdot \Delta_{max} & \text{if } \bar{s_3} \leq s \leq \bar{s_1}, \\ \alpha \cdot \left[1 - |\frac{2 \cdot s - (\bar{s_2} + \bar{s_4})}{\bar{s_4} - \bar{s_2}}|\right] \cdot \Delta_{max} & \text{if } \bar{s_2} \leq s \leq \bar{s_4}, \\ 0 & \text{otherwise.} \end{cases}$$

Here the parameter $\alpha \in I\!R^+$ is used to control the amplitude of the $\Delta(s)$ function. See Figure 14 for the shape of $\Delta(s)$. One can clearly be given control over $\varepsilon_i, i \in \{1, 2, 3, 4\}$, as well as the shape and intensity of the smooth flipping function $\mathcal{F}$, choosing $\xi = \min\{|||R(t_0, \bar{s_1}) - R(t_0, \bar{s_3})||, ||R(t_0, \bar{s_2}) - R(t_0, \bar{s_4})||\}$, $\zeta = \max_i\{\varepsilon_i\}$, and possibly letting the function $\Delta(s)$ to be non-linear, for example a *Bézier* or a *B-spline* function (see Figures 16 and 17).

Finally, note that the two *parallel segments* are translated by $\mathcal{F}$ in the *opposite* directions as s and s_p are exchanging their positions (see Figure 15).

4.2 Continuity of the Flipping Function $\mathcal{F}$

The continuity of the metamorphosis is a necessary requirements. Hence, the flipping function $\mathcal{F}$ must be continuous in both parameters – t and s.

It is obvious that the flipping function $\mathcal{F}$ is continuous as function of the second parameter for any fixed *time* parameter between zero and one (one could select a function $\Delta(s)$ with desired degree of continuity).

The function $\mathcal{F}$ is also continuous as a function of the parameter t for any fixed value of the parameter s for the segment $[t_1, t_2]$, when for every $t_0 \in [t_1, t_2]$ the isoparametric curve $C(s) = R(t_0, s)$, $s \in [0, 1]$ is not simple (self-intersects) or when for each $t_0 \in [t_1, t_2]$ the curve $C(s) = R(t_0, s)$, $s \in [0, 1]$ is simple.

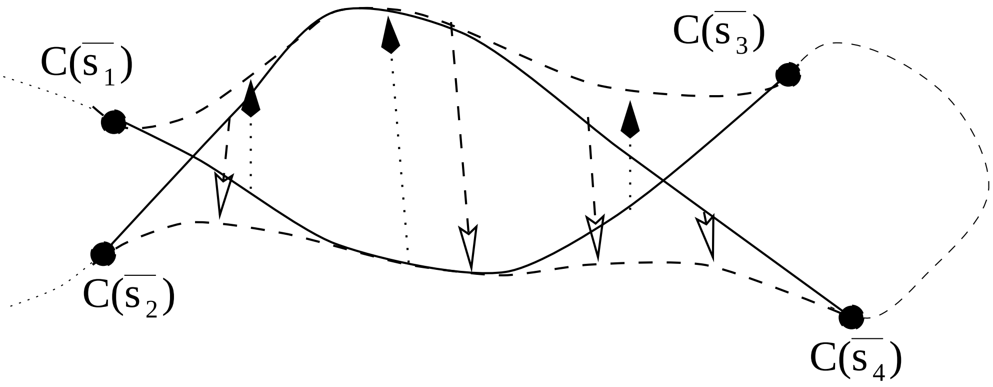

Figure 15: The flipping function $\mathcal{F}$ of the parallel segments of the curve.

Nevertheless the flipping function $\mathcal{F}$ is not continuous on the boundary of the self-intersection region of $R(t, s)$. If an isoparametric curve self-intersects, then the function $\mathcal{F}$ modifies the curve by some amount ξ while $\mathcal{F}$ leaves unmodified self-intersection free isoparametric curves with close t-values. Therefore, one should smoothly interpolate between the isoparametric curves on the boundary of the self-intersection regions, i.e. to treat self-intersection free curves as well, for instance, as long as the offset curves $\bar{C}(s) = C(s) - \frac{\xi}{2} \cdot \vec{N}(s)$ self-intersect, where $\vec{N}(s)$ is the unit normal vector of $C(s)$. If the curve $\bar{C}(s)$ is not simple, than the following curve may be taken as the intermediate curve of the metamorphosis:

$$\tilde{C}(s) = \bar{C}(s) + \frac{\xi}{2} \cdot \Delta_{max} \cdot \vec{N}(s).$$

5 Conclusions

In this article, we have presented two algorithms for correcting self-intersections in the metamorphosis of simple freeform curves. The aim of these algorithms is to eliminate self-intersections in the intermediate curves, which occur during the metamorphosis of two simple planar curves employing convex combination. The first algorithm returns three-dimensional curves as a result of a reparameterization of the *time* in a homotopy that should be projected onto a plane as a post process. The second method returns simple two-dimensional curves at each step of the metamorphosis of the given curves.

One can extend the *Time Variance Algorithm*, and metamorph three-dimensional curves and even freeform surfaces. In the case of metamorphosis of surfaces, one must add one more *time* dimension, and now deal with a trivariate ruled (or possibly even general) *hyper-surfaces* $R(u, v, t)$ in $I\!R^4$. Then, one can construct a similar deformation to the one described in Section 3 and create a self-intersection free morphing in $I\!R^4$. Some projections of the hyper-surfaces into the three-dimensional Euclidean space should be sought, as a second post process step.

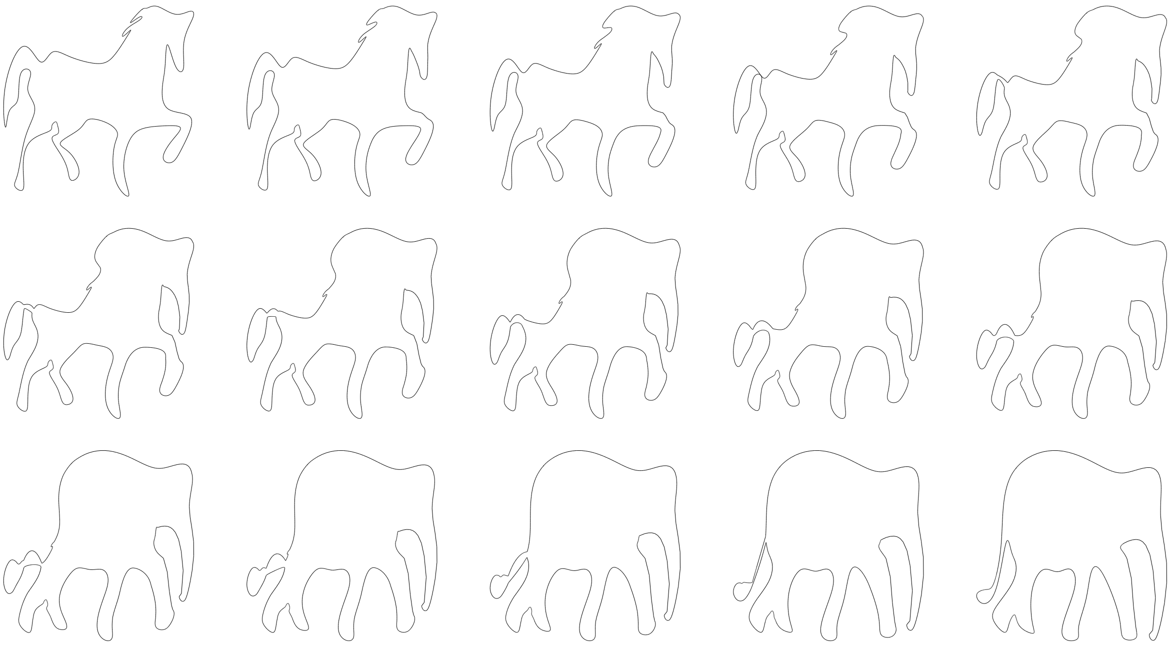

Figure 16: A Morphing sequence between an elephant (bottom right) and a horse (top left), after the *Flipping Algorithm* was used with $\xi = 0.2\%$ of the total curve's length (the minimal arc length between the end points of the parallel segments of the curve) and $\zeta = 0.35\%$ of the total curve's length. $\Delta(s)$ is a cubic Bézier function. Compare with Figures 6 and 17.

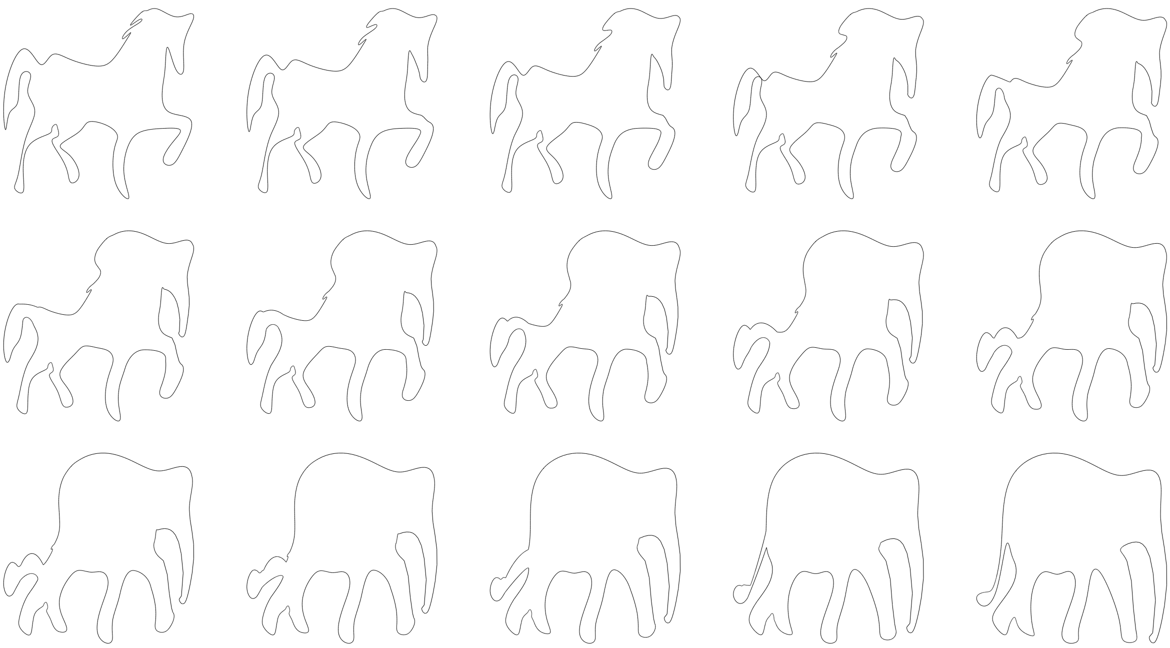

Figure 17: A Morphing sequence between an elephant and a horse, after the *Flipping Algorithm* was used with $\xi = 0.5\%$ and $\zeta = 0.55\%$ of the total curve's length. $\Delta(s)$ is a cubic Bézier function. Compare with Figures 6 and 16.

This work assumed a topological similarity between the two parametric curves, considering simple curves with single loops. The blending of two freeform curves of different topologies continues to be an eluding task.

Finally, one should consider a more general extensions to both *the Flipping and Time Variance Algorithms.* Seeking a general, non linear, surface $S : [0,1] \times [0,1] \longrightarrow \mathbb{R}^3$, with the first *time* parameter t, while employing isoparametric curves $S(t_0, r)$ as the mid-curves of the continuous morphing process. If S can be made self-intersection free, clearly the metamorphosis would be self-intersection free as each isoparametric curve $S(t_0, r)$, $t_0 \equiv const$, $r \in [0,1]$ is self-intersection free.

6 Acknowledgments

The authors are thankful for In Kwon Lee for providing the digitized curves, used in this work, of the elephant and the horse.

This work was supported in part by the Fund for Promotion of Research at the Technion, Haifa, Israel.

References

[1] Beier, T. and Neely, S., 1992. “Feature-Based Image Metamorphosis.” *Computer Graphics (SIGGRAPH '92)*, **26**, pp. 35 - 42.

[2] Cohen, S., Elber, G., and Bar Yehuda, R., 1997. “Matching of Freeform Curves.” *CAD, Vol 29, No 5, pp 369-378. Also Center for Intelligent Systems Tech. Report, CIS 9527, Computer Science Department, Technion.*

[3] Coquillart, S., 1987. “A Control-Point-Based Sweeping Technique.” *IEEE Computer Graphics and Applications*, **7(11)**, pp. 36 - 45.

[4] Do Carmo, M., 1976. “Differential Geometry of Curves and Surfaces.” *Prentice-Hall 1976.*

[5] Elber, G., June 1995. “Metamorphosis of Freeform Curves and Surfaces.” *Computer Graphics Developments in Virtual Worlds, R. A. Earnshaw and J. A. Vince (Eds.), Computer Graphics International 1995 (CGI 95), Leeds, England*, pp 29-40.

[6] Elber, G. and Cohen, E., April 1993. “Second Order Surface Analysis Using Hybrid Symbolic and Numeric Operators.” *Transactions on Graphics,* Vol 12, No 2, pp 160-178.

[7] Goldstein, E. and Gotsman, C., 1995. “Polygon Morphing using a Multiresolution Representation.” *Proceeding of Graphics Interface.* Quebec City.

[8] Hughes, J.F., 1992. "Scheduled Fourier Volume Morphing." *Computer Graphics (SIGGRAPH '92)*, **26**, pp. 43 - 46.

[9] Sederberg, T.W. and Greenwood, E., 1992. "A Physically Based Approach to 2D Shape Blending." *Computer Graphics (SIGGRAPH '92)*, **26**, pp. 25 - 34.

[10] Sederberg, T.W., Gao, P., Wang, G. and Mu, H., 1993. "2D Shape blending: an Intrinsic Solution to the Vertex Path Problem." *Computer Graphics (SIGGRAPH '93)*, **27**, pp. 15 - 18.

[11] Shapira, M. and Rappoport, A., 1994. "Shape Blending using the Star-Skeleton Representation." *Computer Graphics and Application*, Vol. 15, No.2, pp. 44 - 51.

[12] Sun, Y.M., Wang, W. and Chin. F.Y.L., 1994. "Interpolating Polyhedral Models using Intrinsic Shape Parameters." *Computer Graphics (SIGGRAPH '93)*, pp. 133 - 146.